

The Glass "Gravitational" Lens Experiment

Silvia Simionato

Teaching Methodology in Physics and Astronomy RG, Friedrich-Schiller University of Jena (Germany)
silvia.simionato@uni-jena.de

Abstract

Light deflection, in particular the gravitational-lens effect in its strong form, is an interesting and fascinating subject of modern physics and cosmology. Although it is conceptually articulated and complex, it is fortunately possible to approach this topic through a simplified method and analysis, involving different concepts of physics and mathematics typical of the last years of secondary school and first years of the undergraduate studies. The basic idea is the visualisation of light on curved paths under the influence of gravity. In fact, by combining optics and general relativity, it is possible to design plexiglass lenses specifically formulated to reproduce the images of any source, whose light is deflected by different types of celestial objects. The work with these lenses is moreover supported by simulations performed with the software Geogebra and the help of astonishing images from the best telescopes. All this makes gravitational lensing an excellent educational tool for teaching physics and mathematics using examples from astronomy and cosmology.

1. Introduction

When light coming from one or more distant sources passes by a mass distribution positioned between the source and the observer, the light path is bent by the gravitational potential of the mass distribution, from now on called lens. This effect is known as gravitational lensing and the amount of bending was predicted by Albert Einstein's General Theory of Relativity.

The idea arose, however, also in the context of classical physics. This well before Einstein and obviously starting from totally different conceptual assumptions, namely assuming that light consists of material particles, using Newtonian gravity and the Sun as lens. In fact, already Newton hypothesised this effect in his book *Opticks* (1704). Afterwards, Henry Cavendish, in an unpublished note (1783/84), and Johann Georg von Soldner, in a published work from 1801, predicted the amount of the bending of light, but only half of the value derived by the General Relativity [Lotze and Simionato, 2021]. Actually, in his first attempt also Einstein achieved the half of the correct value, this was in 1911 using the equivalence principle. Then in 1915, elaborating and completing his General Theory of Relativity, he corrected this result and for the first time the real amount of light bending was known [Narayan and Bartelmann, 2008]. Einstein's prediction about the deflection of light was proven during the solar eclipse of 29 May 1919 and this was also the first observation of the gravitational-lens effect which made Einstein and his theory famous in the entire world [Lotze and Simionato, 2021].

Einstein was also the first to consider the fact that other stars besides the Sun could act as gravitational lenses and deflect light of distant sources from its original path. But he gave no hope to such observations for basically two reasons. In fact, he considered the necessary alignments between the stars and the observer highly unlikely and, moreover, the order of magnitude of such effects was too small to be actually observed with the instruments of that time [Einstein, 1936]. In this respect, it was in effect the astronomer Fritz Zwicky who in 1937 instead of stars suggested to consider galaxies, called at that time nebulae. Basically, these newly (at that time) defined extragalactic objects had two advantages in the theoretical framework of gravitational lensing: they are much more massive than single stars and they are extended, therefore the necessary alignment is not so improbable anymore [Zwicky, 1937]. However, the real interest in gravitational lensing began in the early 1960s with independent research by S. Refsdal, S. Liebes and Yu. G. Klimov and the contemporary discovery of quasars [Schneider et al., 2006].

Nevertheless, it still took another 15 years before the first gravitational lens system was observed in 1979. Indeed, Walsh, Carswell and Weymann discovered the first gravitational lensing, the quasar QSO 0957+561A,B, nowadays known as the Twin Quasar [Schneider et al., 2006]. And here began a long history of observations and discoveries.

2. Light Deflection and Useful Concepts

At this point we have a basic idea of how gravitational lensing works (fig. 1), however, before ana-

lysing this theme more deeply, we need to introduce some concepts and simplifications used in this article and understand the geometry of the lens system.

First of all, for simplicity and to reach our educational goals without distracting the attention of our students with intricate calculations, all gravitational lenses we consider in our models are axially symmetric.

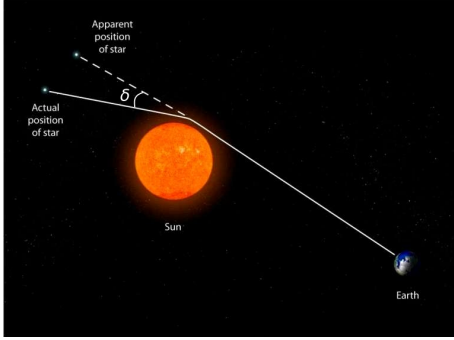


Figure 1: Representation of the gravitational-lens effect (not to scale) of the system consisting of a distant star, the Sun and the Earth. We can see the indicated deflection angle δ . Credit: path2space.com, elaborated by S. Simionato.

Secondly, it is important to know that the amount of bending of the light path, which as we know was predicted by Einstein's General Relativity, is expressed by the deflection angle δ :¹

$$\delta(\theta) = \frac{4G}{c^2} \frac{M(\theta)}{\theta D_L}. \quad (1)$$

Here the ratio $M(\theta)/\theta D_L$ expresses how the angle of deflection is dependent on the mass of the lens and on the impact parameter, namely the shortest distance at which the light ray passes by the lens. In fact, $M(\theta)$, according to Newton's shell theorem, is the mass within the impact parameter b , the only mass that acts gravitationally on the light ray, bending it [Schneider, 2015]. Instead θD_L , as shown in fig. 2, represents the impact parameter b in the lens plane expressed in terms of arc length and under the small-angle approximation. Approximation that we are allowed to use, since the distances involved are much larger than the size of the lens. For this last reason, we also consider that the process of deflection is not continuous, but it happens in a single point close to the lens. This point, distant b from the gravitational lens, and the lens itself define the lens plane. Considering the gravitational lensing happening in a plane brings the consequence that also the entire mass of the lens has to be projected on the same plane, as we will see soon.

From fig. 2, which schematically represents the geometry of the system, we also understand very well that what the observer sees is not the original source,

¹ For the derivation of the deflection angle see [Lotze and Simionato, 2021] and [Lotze, 2020].

but rather images of it deformed in various ways and in different positions.

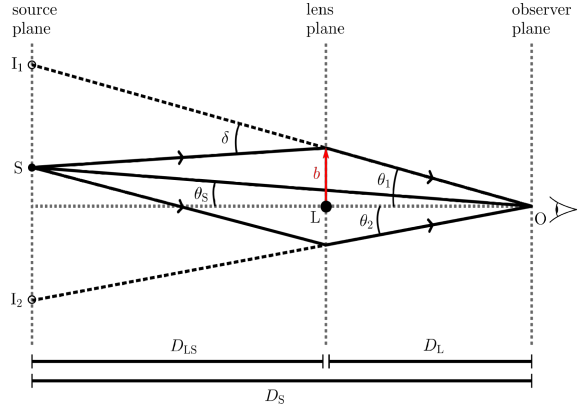


Figure 2: Geometry of the general situation of the gravitational-lens effect. The line connecting observer O and lens L is the starting point for defining the angles that correspond to the position of the source θ_S and the position of the image I_1 on the upper part of the diagram θ_1 . The second image I_2 is on the opposite side of this line. δ is the angle of deflection and b the impact parameter in the lens plane.

These deformations include among other effects also multiple images of the same source, arcs and rings. In this regard, we have to consider the fact that size and shape of the source, different mass distributions for the lens and the relative position of source, lens and observer affect number, position, size and shape of the resulting images. All this together with the geometry of the system is taken into account by the lens equation²

$$\theta - \theta_S - \delta \frac{D_{LS}}{D_S} = 0, \quad (2)$$

whose solution gives us the information about the images. If now we introduce the deflection angle δ (eq.(1)) in eq. (2), we obtain

$$\theta - \theta_S - \frac{4G}{c^2} \frac{M(\theta)}{\theta} \frac{D_{LS}}{D_L D_S} = 0. \quad (3)$$

Thanks to this equation, we are able to describe every possible configuration and deduce important information on the resulting images, the result of the gravitational lensing process. A special case is represented by the perfect alignment of observer, lens and source which occurs when $\theta_S = 0$. In most cases, when facing this situation, the distorted image of the source is a ring around the lens, the so-called Einstein ring. This ring remains constant for each individual configuration. Thus, we can express the lens equation (eq.(3)) in terms of the Einstein ring radius θ_E specific for the considered configuration.

The Einstein ring radius is expressed from eq.(2) by

² For the derivation of the lens equation see [Lotze and Simionato, 2021] and [Lotze, 2020].

$$\theta_E = \frac{4G}{c^2} \frac{M(\theta_E)}{\theta_E} \frac{D_{LS}}{D_L D_S}. \quad (4)$$

Everything we have seen so far is applicable to the real gravitational lens effect that we find in the universe, but also to that resulting from simulations or that can be reproduced in class thanks to special lenses.

The next step requires the projection on the plane of the lens of a mass profile that represents the lens itself. This projected mass will then be introduced instead of $M(\theta)$ in these equations and the result will give us clear information about what the observer sees. At this point it is possible to study many different mass distributions for the lens and observe the corresponding outcomes.

We chose and analysed eight different mass distributions for the lens:

- Point mass lens
- Plummer sphere lens
- Uniform disk lens
- Singular isothermal sphere (SIS) lens
- Kuzmin disk lens
- SIS with a core lens
- Spiral galaxy lens
- Navarro-Frenk-White (NFW) lens.

Among these, the first five have been deeply explored and also designed and produced as plexiglass lenses with the aim of using them as an educational tool in the classroom. In addition, as far as we know, we are the first to have produced the Plummer sphere and Kuzmin disk lenses. The last three were not considered for production as plexiglass lenses because, after a meticulous comparison between them and the Kuzmin disk lens, we discovered a high similarity in the behaviour, the resulting images and the shape of the lenses themselves. Thus, we decided to produce the simplest lens among them with regard to the equations involved and the realization by the university laboratory. In the next paragraph we will discuss two examples of lenses in detail.

3. Different Lenses

Why do we call this effect *gravitational-lens effect*? The name comes from the analogy with "real" lenses we know in optics. In fact, just as lenses deflect light rays due to their refractive power, in the same way, in the universe a massive object, thanks to its gravitational attraction, deflects the rays of light that in a straight line pass near it [Lotze and Simionato, 2021].

Our primary interest falls on galaxies as gravitational lenses. This is because galaxies offer a variety of shapes and internal morphologies and these objects can also be used to trace the distribution of dark matter. The idea is that a galaxy, being made of

stars, has "transparent" space between them, therefore it makes sense to choose an impact parameter inside the galaxy and study the result of the lens equation at different radii, always keeping in mind Newton's shell theorem. Let's see two examples in detail: the famous point mass lens (also known as "foot of a wineglass" -- we'll see why later) and the Plummer sphere lens.

3.1 Point Mass Lens

This case represents the lensing effects produced by gravitational lenses as black holes, massive objects and even stars. In our case it is used for representing galaxies as lenses when observed from very far away. So far away that we can consider them as points and we are able to study around them the effects on light coming from background sources. The main characteristic of this lens is that its mass is independent of θ and concentrated in a point at its centre and the mass density is represented by a Dirac delta function. Thus, we introduce $M(\theta) = M_{\text{tot}}$ in equations (3) and (4) and expressing the result in terms of the Einstein ring radius θ_E (from eq.(4)), we get

$$\theta - \theta_S = \frac{\theta_E^2}{\theta}. \quad (5)$$

Solving eq.(5), we obtain the number and position of produced images from a background point mass source. We can solve this quadratic equation analytically, becoming a nice maths practice, but the easiest way is to solve it graphically, as we did in fig. 3 thanks to the software Geogebra, and analyse then different relative positions of the source.

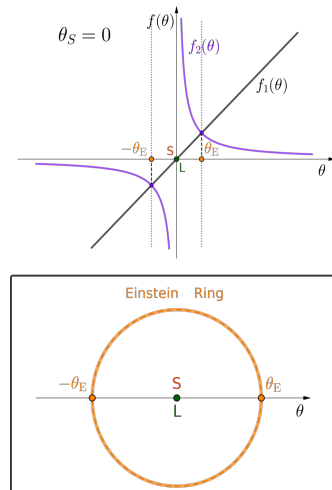


Figure 3: Graphical Geogebra solution of eq.(5) for the point mass lens in the special case of $\theta_S=0$. The observer sees a ring of radius θ_E , the famous Einstein ring, which is shown in the bottom panel.

For the graphical solution we consider the two equations $f_1(\theta) = \theta - \theta_S$ and $f_2(\theta) = \theta_E^2/\theta$. As we see represented in fig. 3, we start with the perfect observer-lens-source alignment, that is $\theta_S=0$, where

for reasons of full symmetry we see a ring of radius θ_E . Then we continue with $\theta_S > 0$ in fig. 4, where the source is considered gradually further and further away from the line joining observer and lens and where we will always see two images of the source.

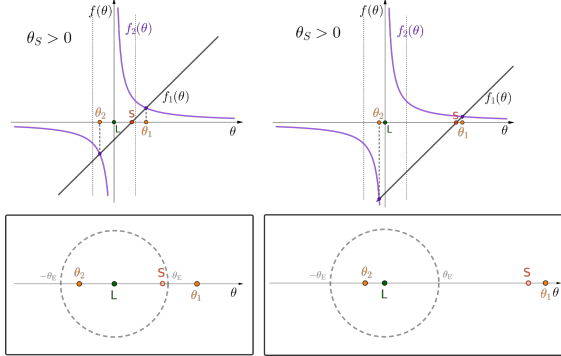


Figure 4: Graphical Geogebra solutions of eq.(5) for the point mass lens in case of $\theta_S > 0$. The observer sees two images, one inside and one outside the Einstein radius θ_E , as shown in the bottom panel. The further away the source is from the lens, as seen in projection, the closer the image will be to the source itself and the other to the lens, the latter two arrive in extreme cases to merge so that they cannot be distinguished.

One image is positioned inside θ_E and the other outside. Moreover, the further the source moves away from the lens, as seen in projection, the closer the internal image gets to the lens itself, eventually merging with it, and the further the external image moves away.

The next stage in this process is to consider different types of source, for instance an extended source, and to solve the lens equation for each point of the source in order to obtain the images produced by the lens. We did this using Geogebra for an extended disk source and also for a line source.

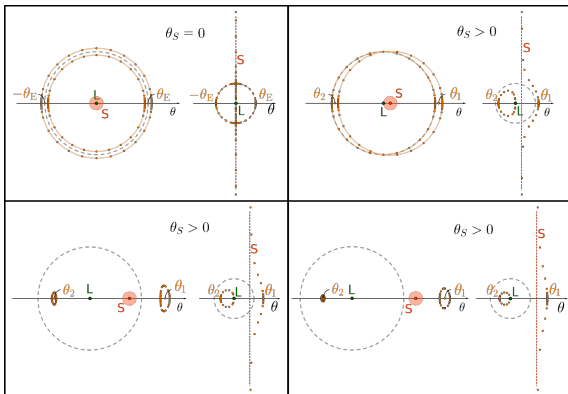


Figure 5: Simulation with Geogebra of the solution of the lens equation for the point mass lens in the case of an extended disk and a line as sources, indicated with S. The sequence starts with the upper left panel, where $\theta_S = 0$, then going right and bottom left, then right again we see the sources S moving sideways away from the lens L. The dots represent the produced images of specific points of the sources and give us an idea of the total images shape.

The images of the sources central point along the θ -axis are always indicated with θ_1 and θ_2 .

As for the disk, the lens equation is applied to the central point and various points of the circular edge, while for the line, it is applied to various points along the line. The result for some relative source-observer positions is shown in fig. 5.

3.2 Plummer Sphere Lens

The next case represents the lensing effects produced by galaxies or clusters of stars. The model for this lens, invented in 1911 [Plummer, 1911], approximates a spherical halo, in fact the mass is distributed in an infinite sphere with a finite density core and it falls off as r^{-5} at large radii. Actually it falls steeper than in a real galaxy, nevertheless this model is widely used in N-body simulations of stellar systems [Sellwood, 2015]. Typical for this lens is the fact that the total mass is reached at infinity and there is a scale radius a which roughly represents the halo radius, in fact after this radius the gravitational potential is similar to that of a point mass. Since, as said, we need to project the lens mass on the lens plane, we consider the mass density and mass radial profiles in three dimensions first and in two dimensions afterwards. Therefore we get

$$\begin{aligned} \mu(r) &= \frac{3a^2 M_{\text{tot}}}{4\pi(r^2 + a^2)^{5/2}} \\ \rightarrow \sigma(\rho) &= \frac{a^2 M_{\text{tot}}}{\pi(\rho^2 + a^2)^2}, \end{aligned} \quad (6)$$

where r in the mass density profile $\mu(r)$ represents the distance from the lens centre in space and ρ in the surface mass density profile $\sigma(\rho)$ represents this distance in the lens plane instead. M_{tot} is the total mass of the lens reached at infinity. Thus calculating the mass profile we obtain

$$\begin{aligned} M(r) &= \frac{r^3 M_{\text{tot}}}{(r^2 + a^2)^{3/2}} \\ \rightarrow M(\rho) &= \frac{\rho^2 M_{\text{tot}}}{\rho^2 + a^2}, \end{aligned} \quad (7)$$

here $M(\rho)$ is the searched projected mass that we have to use in the lens equation. Indeed, as we did for the point mass lens, we introduce now the projected mass from eq.(7) in equations (3) and (4) and again expressing the result in terms of the Einstein radius θ_E (from eq.(4)),³ we obtain

$$\theta - \theta_S = \theta \frac{\theta_E^2 + \theta_a^2}{\theta^2 + \theta_a^2}. \quad (8)$$

³ Notice that $\rho = \theta D_L$ and $a = \theta_a D_L$.

Also in this case, solving eq.(8) we obtain the number and position of produced images from a background point mass source. The analytical solution involves a cubic equation, which engages students in a nice calculation, but again the easiest solution is graphical (fig. 6).

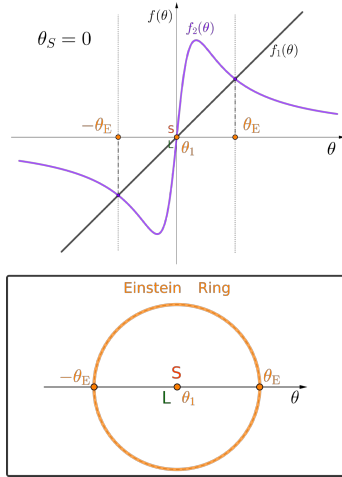


Figure 6: Graphical Geogebra solution of eq.(8) for the Plummer sphere lens in the special case of $\theta_S=0$. In this case the observer sees the Einstein ring of radius θ_E and a central image, as shown in the bottom panel.

For this lens the two equations considered for the graphical solution are $f_1(\theta)=\theta-\theta_S$ and

$$f_2(\theta)=\theta \frac{\theta_E^2 + \theta_a^2}{\theta^2 + \theta_a^2} .$$

In fig. 6, the perfect observer-lens-source alignment is shown, where we not only see a ring of radius θ_E , but also a central point-like image. Then we continue with $\theta_S>0$ in fig. 7, where the source is considered gradually further and further away from the line joining observer and lens. This time, depending on how far away the source is from the lens, we will see respectively three, two or one image of the source.

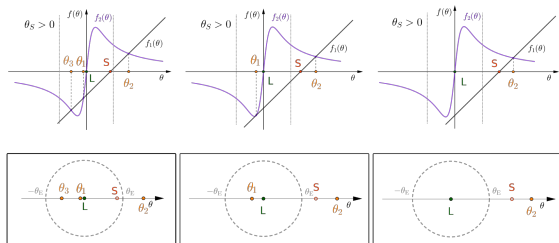


Figure 7: Graphical Geogebra solutions of eq.(8) for the Plummer sphere lens in case of $\theta_S>0$. The observer sees at first three images, two inside and one outside the Einstein radius θ_E , as shown in the left bottom panel. The further away the source is, as seen in projection, the closer one image will be to the source itself. The other two instead move towards each other, until they merge together into a single image (central panel), then disappear (right panel).

We can of course apply this procedure to different kinds of sources, as done before, and some results for the extended disk source are shown in fig. 8.

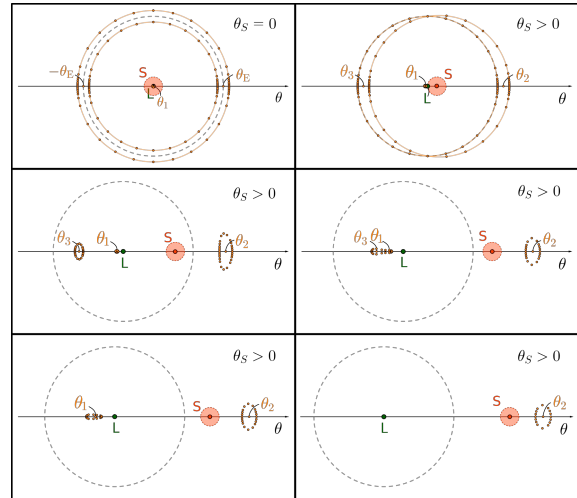


Figure 8: Simulation with Geogebra of the solution of the lens equation for the Plummer sphere lens in the case of an extended disk S as source. We can follow the sequence always from left to right and going then down. The sequence starts with the upper left panel, where $\theta_S=0$, then we see the source S moving sideways away from the lens L. The dots represent the produced images of specific points of the source and give us an idea of the total images shape. The images of the source central point along the θ -axis are always indicated with θ_1 , θ_2 and θ_3 .

4. The Plexiglass Lens Shape

An interesting question we can ask ourselves is: how is it possible to visualize the gravitational-lens effect? This is the question that the Norwegian astrophysicist Refsdal wanted to answer in the 1960s, when still no gravitational lens had been detected (the first extragalactic detection was in 1979 with the Twin Quasar). So apparently the idea of combining optics and general relativity with the aim of producing glass lenses capable of showing us the effects of gravitational lensing was born. It seems indeed that the first to produce the point mass lens was precisely Refsdal at the University of Hamburg [Refsdal and Surdej, 1994]. The modern answer to this question is clear, it is just enough searching through the stunning photos of the Hubble Space Telescope (HST) or other powerful telescopes and observing the gravitational lenses that nature offers us. However, an alternative, which has also proved to be a useful educational tool in explaining this topic with an experimental part, is represented by these special plexiglass lenses. The maximum result is actually obtained by joining these two possibilities.

Obviously, these lenses must have a special profile to reproduce gravitational lensing in a physically correct way. So how can we understand what shape the plexiglass lens must have in order to represent and simulate the effects of a certain mass distribu-

tion? For answering this question we need to combine what we know from general relativity and optics. This procedure is not so complex as it seems. In fact, from experience, it is feasible to perform it with students of the last years of secondary school, especially if they are particularly interested in the subject. Thus, referring to fig. 9, we apply now this method and extrapolate the profile for the plexiglass lenses representing a point mass and a Plummer sphere distribution of mass. These lenses will reproduce the images we saw in the first part of this article.

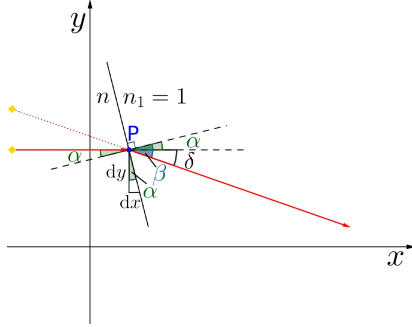


Figure 9: Geometry of the deflection of a light ray traveling through two mediums with different refractive index n , $n_1=1$ is air, according to Snell's law and introducing the concept of deflection angle δ .

First of all, one side of our plexiglass lens is flat for simplicity and we have to infer the shape for the other side. Secondly, our lenses are rotationally symmetric, therefore it is enough to calculate the profile in two dimensions and then rotating it around a central axis we get the entire lens. Indeed, this simplifies our work considerably. The inclined black line in fig. 9 represents the tangent line to the surface of the plexiglass lens in the point P, if we can understand how the tangent line changes for all points of the lens, it is possible to find the corresponding function which describes the shape of the lens. Basically, what we need is the deflection angle δ from General Relativity and Snell's law from optics. Let's start analysing fig. 9 and introducing these concepts. We know that, when passing near a massive object, the path of a light ray from a distant source is deflected. This path is represented by the red arrows in the diagram. The amount of deflection, as we know and as it is shown in the figure, is represented by the deflection angle δ expressed by eq.(1). If we now apply Snell's law to this configuration and make use of the trigonometric angle sum and difference identities,⁴ we obtain

$$n = \frac{\sin(\alpha + \delta)}{\sin \alpha} = \cos \delta + \cot \alpha \sin \delta. \quad (9)$$

From eq.(9), inserting eq.(1) for the angle δ , and from considering the diagram, we see that

⁴ $\sin(\alpha \pm \beta) = \sin \alpha \cos \beta \pm \sin \beta \cos \alpha$.

$$\frac{dy}{dx} = -\cot \alpha = -\frac{n - \cos \delta}{\sin \delta} \quad \text{and}$$

$$\frac{dy}{dx} \approx -\frac{n-1}{\delta} = -\frac{(n-1)c^2}{4GM(y)} \cdot y, \quad (10)$$

where δ is expressed by y instead of θ with $y = \theta D_L$ and the small-angle approximation is used. At this point, solving this differential equation with the desired mass distribution inserted in the place of $M(y)$ gives the profile of the corresponding lens. Indeed, for mass distributions not too complicated, this differential equation is easily solved separating the variables and integrating.

4.1 Point Mass Lens

Thus, knowing that the point mass has constant mass M_{tot} , eq.(10) becomes

$$\frac{dy}{dx} = -\frac{(n-1)c^2}{4GM_{\text{tot}}} \cdot y. \quad (11)$$

Then solving it for a generic lens, we obtain

$$y = A e^{-\frac{(n-1)c^2}{4GM_{\text{tot}}} \cdot x}, \quad (12)$$

whose exponential function defines the shape of the lens as in fig. 10 and A is a constant.

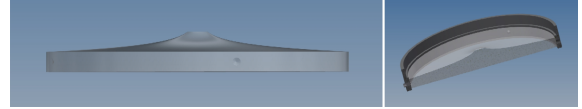


Figure 10: Point mass plexiglass lens profile. Credit: T.Köhler.

From this particular shape comes also the name "foot of a wineglass" lens. Even though the shape of a real wine glass foot is not an exponential function, it is still very similar and even the images it produces are in strong resemblance with the ones produced by this type of lens. Therefore, remembering we do not know what kind of mass distribution it represents and not even if what it represents is real, we can from a qualitative point of view use the foot of a wine glass to have a rough, but accessible to everyone, simulation of this kind of gravitational lens.

4.2 Plummer Sphere Lens

For this lens we insert the projected mass from eq. (7) at the place of the mass $M(y)$ in eq.(10), obtaining

$$\frac{dy}{dx} = -\frac{(n-1)c^2}{4GM_{\text{tot}}} \frac{y^2 + a^2}{y}. \quad (13)$$

Solving it again for a generic lens, we have

$$y = \sqrt{A \cdot e^{-2 \frac{(n-1)c^2}{4GM_{\text{tot}}} \cdot x} - a^2}, \quad (14)$$

whose shape is shown in fig. 11 and A is again a constant.

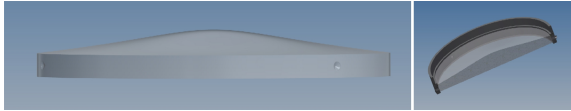


Figure 11: Plummer sphere plexiglass lens profile. Credit: T. Köhler

5. Experimenting

At this point we can spend some words on how to use the lenses in the classroom and what possibilities they give us from an experimental point of view, alongside the theoretical explanation. Ultimately, the plexiglass lenses that reproduce gravitational lensing effects are suitable to be used in two different configurations:

- It is in fact possible to shine light at the lens, better if the light rays from the source are collimated, and observe the resulting effects on a screen behind a shield with a pinhole which represents the observer.
- Alternatively, we can look at a source through the lens using simply our eyes or a camera. The source can be anything (a point, a disk, a word, a picture, etc.) and better if illuminated with light for a better view.

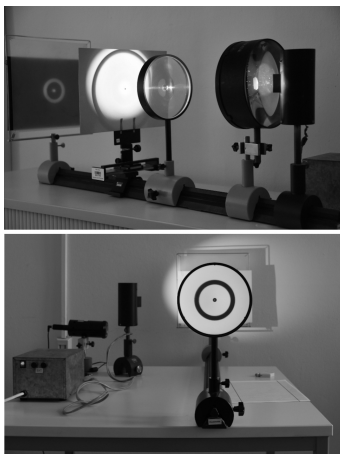


Figure 12: The two setups that can be used with the plexiglass lenses (here the Plummer sphere lens). Upper: Light is shined at the lens. Bottom: The observer looks at a source (a black disk) through the lens.

The two setups are shown in fig. 12 and both these setups are good for working with the lenses, however we personally prefer the second one because it allows a great variety of images to be used as sources and we are able to easily produce pictures and videos. This way we can see many effects and test the lenses with the most different images as sources. It also becomes a fun way to "play" with the

lenses and engage students without making them lose their attention. Moreover, it is also interesting to compare the gravitational lens effects that we produce thanks to the lenses with real ones or even with the Geogebra simulations. Few examples are in figures 13, 14, 15 and 16.



Figure 13: Example of Einstein rings. In the centre the lensed galaxy "Cosmic Horseshoe", on the left side the Plummer sphere lens in action with a disk source and on the right side the point mass lens in action with a point source. Credit for the central image: ESA/Hubble NASA.

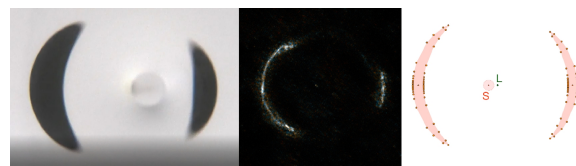


Figure 14: Example of arcs. In the centre the lensed galaxy SDP.81, on the left side the point mass lens in action with a disk source and on the right side a Geogebra simulation with a disk source. Credit for the central image: ALMA.

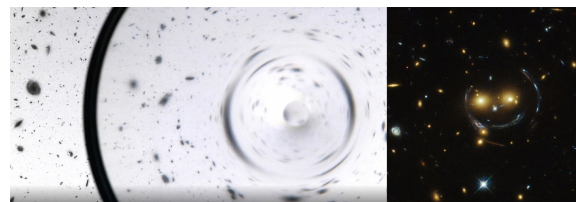


Figure 15: The Hubble Ultra Deep Field (Credit:ESA/Hubble NASA) seen through the point mass lens on the left. The lensed group of galaxies "Cheshire Cat" on the right. Credit for the right image: NASA/STScI.

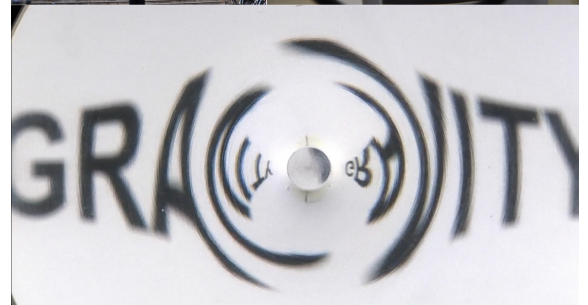


Figure 16: Playing with the lenses. Upper: (left) our faculty building through the Plummer sphere lens, (right) a

portrait of Einstein through the point mass lens. Bottom: the word "GRAVITY" through the point mass lens, inspired by [Gott, 1983]. This last picture shows how images seen through the lenses can also be reversed.

6. Conclusions

These lenses are powerful educational tools to teach the phenomenon of light deflection due to weak gravitational fields and in particular gravitational lensing. They integrate very well the theory with an experimental part that can also, but not compulsorily, allow to practice some mathematical concepts.

The reasons that have led us to deal with this topic are many. First of all, it is a fascinating and modern subject that we often hear about. It is also interesting to think that what we see in the universe with our own eyes does not necessarily reflect the real situation. This topic also offers the possibility to use a simplified model and approximations that make it suitable for students of the last years of secondary school. We would like also to emphasise the fact that all of the physical and mathematical concepts involved are absolutely understandable and practicable by students at this level and in this specific case they are taught applied to a concrete example, a practice that is known to raise the students' level of interest and their ability in scientific subjects [Prince and Felder, 2006]. Not only that, but the use of these lenses in teaching gives a certain added value because it combines an experimental part with a subject that frequently is treated in a pure theoretical way. Therefore, by involving students in these activities, we make them active learners and not simply passive listeners, promoting longer lasting learning and the development of important skills such as problem solving, critical and creative thinking and adaptability [Simionato, 2013].

Acknowledgement

My first and most heartfelt thanks go to Karl-Heinz Lotze for the stimulating discussions and appreciated advice, but above all because without him none of this would have been possible. Many thanks also to the colleagues who helped and supported us to make what was only on paper in plexiglass: Bernard Klumbies and Martin Huber from the university lab and Thomas Köhler for the computer design work. And thanks to Thomas Schott for the useful assistance with the videos.

7. Literature

- Einstein, A. (1936). Lens-like action of a star by the deviation of light in the gravitational field. *Science*, 84(2188):506–507.
- Gott, J. R. (1983). Gravitational Lenses: Cosmic mirages produced by gravitational bending of light may solve some of the most pressing problems in cosmology today. *American scientist*, 71(2):150–157.
- Lotze, K.-H. (2020). Various approaches to teach light deflection in gravitational fields. *Proceedings of the Jena 2019 Heraeus Summer School "Astronomy from 4 Perspectives"*.
- Lotze, K.-H. and Simionato, S. (2021). *Gravitational Lensing as Focal Point for Teaching General Relativity*. Chapter from the book: *Teaching Einsteinian Physics in Schools*. In preparation. Taylor & Francis.
- Narayan, R. and Bartelmann, M. (2008). Lectures on gravitational lensing. *arXiv preprint astro-ph/9606001 [27.04.2020]*.
- Plummer, H. C. (1911). On the problem of distribution in globular star clusters. *Monthly notices of the royal astronomical society*, 71:460–470.
- Prince, M. J. and Felder, R. M. (2006). Inductive teaching and learning methods: Definitions, comparisons, and research bases. *Journal of engineering education*, 95(2):123–138.
- Refsdal, S. and Surdej, J. (1994). Gravitational lenses. *Reports on Progress in Physics*, 56:117–185.
- Schneider, P. (2015). *Extragalactic astronomy and cosmology: an introduction*. Springer.
- Schneider, P., Kochanek, C., and Wambsganss, J. (2006). *Gravitational lensing: strong, weak and micro*. Springer.
- Sellwood, J. (2015). Relaxation in N-body simulations of spherical systems. *Monthly Notices of the Royal Astronomical Society*, 453(3):2919–2926.
- Simionato, S. (2013). Development of Astronomy Educational Resources: the Case of "Universe Awareness". Master Thesis, University of Padua.
- Zwicky, F. (1937). Nebulae as gravitational lenses. *Physical Review*, 51(4):290.